A Sliding Mode Control associated to the Field-Oriented Control of Dual-Stator Induction Motor Drives

Hocine Amimeur, Rachid Abdessemed, Djamal Aouzellag, Elkheir Merabet and Farid Hamoudi

***Abstract*— A sliding mode control strategy associated to the field-oriented control of dual-stator induction motor drives is discussed in this paper. The induction machine has two sets of stator three-phase windings spatially shifted by 30 electrical degrees. The sliding mode control is a robust non linear algorithm which uses discontinuous control to force the system states trajectories to join some specified sliding surface. It has been widely used for its robustness to model parameter uncertainties and external disturbances. The simulation results are presented.**

***Index Terms*— Field-Oriented Control (FOC), Dual-Stator Induction Motor Drives (DSIM), Sliding Mode Control (SMC).**

I. Introduction

INVENTED by Nikola Tesla in 1888, the alternating-current (AC) induction motor has had a major role in the development of the electrical industry [1]. The primary advantages of induction machine are less maintenance cost, brushless construction (squirrel-cage rotor), better transient, etc.

Since the late 1920s, dual-stator AC machines have been used in many applications (such as: pumps, fans, compressors, rolling mills, cement mills, mine hoists [2]), for their advantages in power segmentation, reliability, lower torque pulsations, less dc-link current harmonics, reduced rotor harmonics and higher power per ampere ratio for the same machine volume, etc. [3] – [6].

The sliding mode control theory was proposed by Utkin in 1977 [7]. Thereafter, the theoretical works and its applications of the sliding mode controller were developed. Since the robustness is the best advantage of a sliding mode control, it has been widely employed to control nonlinear systems, especially the systems that have model uncertainty and external disturbance [8], [9]. These advantages justify the necessity of applying this kind of control for the DSIM.

The paper is organized as follows. Description of the DSIM and the mathematical model are provides in Section II. The field oriented control of an DSIM is developed in Section III. The sliding mode control theory is presented in Section IV. The sliding mode control of an DSIM is developed in Section V and its proprieties are validated through simulation results in Section VI. Finally, Section VII summarizes conclusions.

H. Amimeur, R. Abdessemed, E. Merabet and F. Hamoudi are with the group LEB-Research Laboratory, Department of Electrical Engineering, University of Batna. Street Chahid Mohamed El hadi Boukhlouf, 05000, Batna, Algeria (e-mail: amimeurhocine2002@yahoo.fr; r.abdessemed@lycos.com; merabet_elkheir@yahoo.fr; f_hamoudi@yahoo.fr).

D. Aouzellag was with Electrical Engineering Department, A. Mira University, Bejaia, Algeria (e-mail: aouzellag@hotmail.com).

II. Machine Model

A schematic of the stator and rotor windings for a dual-stator induction machine is given in Fig. 1. The six stator phases are divided into two wye-connected three-phase sets, labled (a_{s1}, b_{s1}, c_{s1}) and (a_{s2}, b_{s2}, c_{s2}), whose magnetic axes are displaced by $\alpha = 30$ electrical angle. The windings of each three-phase set are uniformly distributed and have axes that are displaced 120 apart. The three-phase rotor windings (a_r, b_r, c_r) are also sinusoidally distributed and have axes that are displaced by 120 apart [10] – [12].

The following assumptions have been made in deriving the dual-stator induction machine model:

- Machine windings are sinusoidally distributed;
- The two stars have same parameters;
- Flux path is linear;
- The magnetic saturation and the mutual leakage are neglected.

The electrical equations of the dual-stator induction motor drives in the synchronous reference frame $(d-q)$ are given

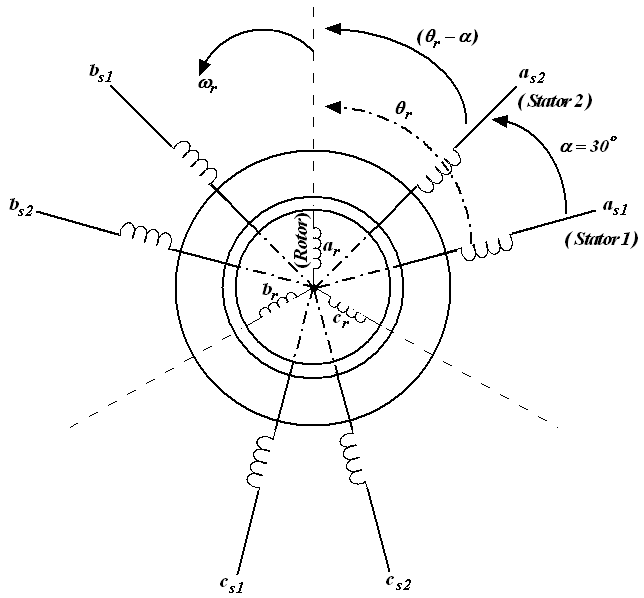

Fig. 1. Dual-stator windings induction machine.

as [13] – [15]

$$v_{d1} = r_1 \imath_{d1} + p\psi_{d1} - \omega_e \psi_{q1} \quad (1)$$
$$v_{q1} = r_1 \imath_{q1} + p\psi_{q1} + \omega_e \psi_{d1} \quad (2)$$
$$v_{d2} = r_2 \imath_{d2} + p\psi_{d2} - \omega_e \psi_{q2} \quad (3)$$
$$v_{q2} = r_2 \imath_{q2} + p\psi_{q2} + \omega_e \psi_{d2} \quad (4)$$
$$v_{dr} = r_r \imath_{dr} + p\psi_{dr} - (\omega_e - \omega_r)\psi_{qr} = 0 \quad (5)$$
$$v_{qr} = r_r \imath_{qr} + p\psi_{qr} + (\omega_e - \omega_r)\psi_{dr} = 0 \quad (6)$$

with,
v_{d1}, v_{d2}, $\imath_{d1}$, $\imath_{d2}$, and ψ_{d1}, ψ_{d2} are respectively the "d" components of the stator voltages, currents and flux linkage;
v_{q1}, v_{q2}, $\imath_{q1}$, $\imath_{q2}$, and ψ_{q1}, ψ_{q2} are respectively the "q" components of the stator voltages, currents and flux linkage;
v_{dr}, $\imath_{dr}$ and ψ_{dr} are respectively the "d" components of the rotor voltage, current and flux linkage;
v_{qr}, $\imath_{qr}$ and ψ_{qr} are respectively the "q" components of the rotor voltage, current and flux linkage;
r_1, r_2 and r_r are respectively the per phase stator resistance and the per phase rotor resistance;
ω_e is the speed of the synchronous reference frame;
ω_r is the rotor electrical angular speed;
p denotes differentiation $w.r.t$ time.

The expressions for stator and rotor flux linkages are

$$\psi_{d1} = L_1 \imath_{d1} + L_m(\imath_{d1} + \imath_{d2} + \imath_{dr}) \quad (7)$$
$$\psi_{q1} = L_1 \imath_{q1} + L_m(\imath_{q1} + \imath_{q2} + \imath_{qr}) \quad (8)$$
$$\psi_{d2} = L_2 \imath_{d2} + L_m(\imath_{d1} + \imath_{d2} + \imath_{dr}) \quad (9)$$
$$\psi_{q2} = L_2 \imath_{q2} + L_m(\imath_{q1} + \imath_{q2} + \imath_{qr}) \quad (10)$$
$$\psi_{dr} = L_r \imath_{dr} + L_m(\imath_{d1} + \imath_{d2} + \imath_{dr}) \quad (11)$$
$$\psi_{qr} = L_r \imath_{qr} + L_m(\imath_{q1} + \imath_{q2} + \imath_{qr}) \quad (12)$$

where,
L_1, L_2 and L_r are respectively the per phase stator self inductance and the per phase rotor self inductance;
L_m is the mutual inductance between stator and rotor.

The electromagnetic torque is evaluated as

$$T_{em} = P\frac{L_m}{L_m + L_r}\left[(\imath_{q1} + \imath_{q2})\psi_{dr} - (\imath_{d1} + \imath_{d2})\psi_{qr}\right] \quad (13)$$

with, P is the number of pole pairs.

The mechanical equation of machine is described as

$$Jp\Omega + f\Omega = T_{em} - T_L \quad (14)$$

where,
Ω is the mechanical speed ($\Omega = \frac{\omega_r}{P}$);
T_L is the load torque;
J is the moment of inertia;
f is the viscous bearing friction coefficient.

III. Field Oriented Control of an DSIM

The main objective of the vector control of induction motors is, as in DC machines, to independently control the torque and the flux [16]. In this order, we propose to study the FOC of the DSIM. The control strategy used consist to maintain the quadrature component of the flux null ($\psi_{qr} = 0$) and the direct flux equals to the reference ($\psi_{dr} = \psi_r^*$):

$$\psi_{dr} = \psi_r^* \quad (15)$$
$$\psi_{qr} = 0 \quad (16)$$
$$p\psi_r^* = 0 \quad (17)$$

Substituting Eqs. (15), (16) and (17) into Eqs. (5) and (6), yields

$$r_r \imath_{dr} + p\psi_r^* = 0 \Rightarrow \imath_{dr} = 0 \quad (18)$$

$$r_r \imath_{qr} + \omega_{sl}^* \psi_r^* = 0 \Rightarrow \imath_{qr} = -\frac{\omega_{sl}^* \psi_r^*}{r_r} \quad (19)$$

with, $\omega_{sl}^* = \omega_e^* - \omega_r$, ($\omega_{sl}$ is the slip speed).

The rotor currents in terms of the stator currents are divided from Eqs. (11) and (12) as

$$\imath_{dr} = \frac{1}{L_m + L_r}\left[\psi_r^* - L_m(\imath_{d1} + \imath_{d2})\right] \quad (20)$$

$$\imath_{qr} = -\frac{L_m}{L_m + L_r}(\imath_{q1} + \imath_{q2}) \quad (21)$$

Substituting Eq. (21) into (19), obtain

$$\omega_{sl}^* = \frac{r_r L_m}{(L_m + L_r)}\frac{(\imath_{q1} + \imath_{q2})}{\psi_r^*} \quad (22)$$

The final expression of the electromagnetic torque is

$$T_{em}^* = \frac{PL_m}{(L_m + L_r)}(\imath_{q1} + \imath_{q2})\psi_r^* \quad (23)$$

With taking into the rotor field orientation, the stator voltage equations (1)–(4) can be rewritten as

$$v_{d1}^* = r_1 \imath_{d1} + L_1 p\imath_{d1} - \omega_e^*(L_1 \imath_{q1} + \tau_r \psi_r^* \omega_{sl}^*) \quad (24)$$
$$v_{q1}^* = r_1 \imath_{q1} + L_1 p\imath_{q1} + \omega_e^*(L_1 \imath_{d1} + \psi_r^*) \quad (25)$$
$$v_{d2}^* = r_2 \imath_{d2} + L_2 p\imath_{d2} - \omega_e^*(L_2 \imath_{q2} + \tau_r \psi_r^* \omega_{sl}^*) \quad (26)$$
$$v_{q2}^* = r_2 \imath_{q2} + L_2 p\imath_{q2} + \omega_e^*(L_2 \imath_{d2} + \psi_r^*) \quad (27)$$

where, $\tau_r = \frac{L_r}{r_r}$ is time rotor constant.

Consequently, the electrical and mechanical equations for the system after these transformations in the space control may be written as follows

$$p\imath_{d1} = \frac{1}{L_1}\left\{v_{d1}^* - r_1 \imath_{d1} + \omega_e^*(L_1 \imath_{q1} + \tau_r \psi_r^* \omega_{sl}^*)\right\} \quad (28)$$

$$p\imath_{q1} = \frac{1}{L_1}\left\{v_{q1}^* - r_1 \imath_{q1} - \omega_e^*(L_1 \imath_{d1} + \psi_r^*)\right\} \quad (29)$$

$$p\imath_{d2} = \frac{1}{L_2}\left\{v_{d2}^* - r_2 \imath_{d2} + \omega_e^*(L_2 \imath_{q2} + \tau_r \psi_r^* \omega_{sl}^*)\right\} \quad (30)$$

$$p\imath_{q2} = \frac{1}{L_2}\left\{v_{q2}^* - r_2 \imath_{q2} - \omega_e^*(L_2 \imath_{d2} + \psi_r^*)\right\} \quad (31)$$

$$p\psi_r = -\frac{r_r}{L_r + L_m}\psi_r + \frac{r_r L_m}{L_r + L_m}(\imath_{d1} + \imath_{d2}) \quad (32)$$

$$p\Omega = \frac{1}{J}\left\{P\frac{L_m}{L_r + L_m}(\imath_{q1} + \imath_{q2})\psi_r^* - T_r - f\Omega\right\} \quad (33)$$

IV. Sliding Mode Control

We consider a system described by the following state space equation:

$$[\dot{X}] = [A][X] + [B][U] \tag{34}$$

with,
$[X] \in \mathbb{R}^n$ is the state vector;
$[U] \in \mathbb{R}^m$ is the control input vector;
$[A]$ and $[B]$ are system parameter matrices.

The first phase of the control design consist to choose the number of the switching surfaces $S(x)$. Generally this number is equal the dimension of the control vector U. In order to ensure to convergence of the state variable x to its reference value x^*, [8], [16] and [17] propose a general function of the switching surface:

$$S(x) = (\frac{d}{dt} + \lambda)^{r-1} e(x) \tag{35}$$

where,
λ is a strictly positive constant;
r is the smallest positive integer such that $\frac{\partial \dot{S}}{\partial U} \neq 0$: ensure controllability;
$e(x) = x^* - x$ is the error variable.

The second phase consists to find the control law which meets the sufficiency conditions for the existence and reachibility of a sliding mode such as [7], [17], [18]

$$S(x)\dot{S}(x) < 0 \tag{36}$$

Intuitively, the existence of a sliding mode on the sliding surface implies stability of the system. One of the possible solutions is given by

$$U_c = U_{eq} + U_n \tag{37}$$

U_{eq} is the so called equivalent control. It plays the feedback linearisation role is the solution of

$$\dot{S}(x) = 0 \Leftrightarrow \frac{\partial S}{\partial X}\{[A][X] + [B]U_{eq}\} + \frac{\partial S}{\partial X}[B]U_n = 0 \tag{38}$$

During the sliding mode, the U_n is equal zero, then U_{eq} is

$$U_{eq} = -\left\{\frac{\partial S}{\partial X}[B]\right\}^{-1}\left\{\frac{\partial S}{\partial X}[A][X]\right\} \tag{39}$$

with

$$\frac{\partial S}{\partial X}[B] \neq 0 \tag{40}$$

During the convergence mode, the $U_n \neq 0$. We substituting Eq. (39) into Eq. (38) yields

$$\dot{S}(x) = \frac{\partial S}{\partial X}[B]U_n \tag{41}$$

Substituting Eq. (41) into Eq. (36), obtain

$$S(x)\frac{\partial S}{\partial X}[B]U_n < 0 \tag{42}$$

So that the state trajectory be attracted to the switching surface $S(x) = 0$. A commonly used from of U_n is a constant relay control [17].

$$U_n = k_x sgn(S(x)) \tag{43}$$

$sgn(S(x))$ is a sign function, which is defined as

$$sgn(S(x)) = \begin{cases} -1 & \text{if} \quad S(x) < 0 \\ 1 & \text{if} \quad S(x) > 0 \end{cases} \tag{44}$$

k_x is a constant.

This introduces some undesirable chattering. Hence, we will substitute it by the function plotted in Fig. 2.
Consequently, U_n is defined as

$$U_n = k_x \frac{S(x)}{|S(x)| + \xi_x} \tag{45}$$

ξ_x is small positive scalar.

V. Sliding Mode Control of an DSIM

The proposed control scheme is a cascade structure at it is shown in Fig. 3, in which six surfaces are required. The internal loops allow the control stator current components ($\imath_{d1}$, $\imath_{q1}$, $\imath_{d2}$ and $\imath_{q2}$), whereas the external loops provide the regulation of the speed Ω and the flux ψ_r. The bloc of the FOC(SMC) is presented in Fig. 4.

A. Design of the Switching Surfaces

In this work, six sliding surfaces are used and taken as follows since a first order is used:

$$S(\Omega) = \Omega^* - \Omega \tag{46}$$

$$S(\psi_r) = \psi_r^* - \psi_r \tag{47}$$

$$S(\imath_{d1}) = \imath_{d1}^* - \imath_{d1} \tag{48}$$

$$S(\imath_{q1}) = \imath_{q1}^* - \imath_{q1} \tag{49}$$

$$S(\imath_{d2}) = \imath_{d2}^* - \imath_{d2} \tag{50}$$

$$S(\imath_{q2}) = \imath_{q2}^* - \imath_{q2} \tag{51}$$

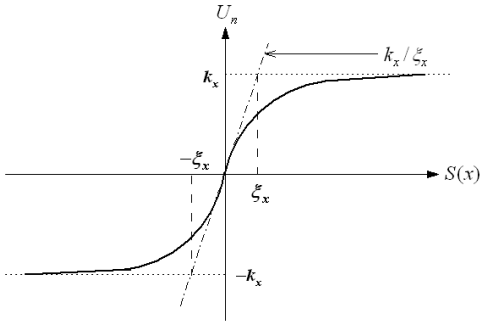

Fig. 2. Shape of the sgn function.

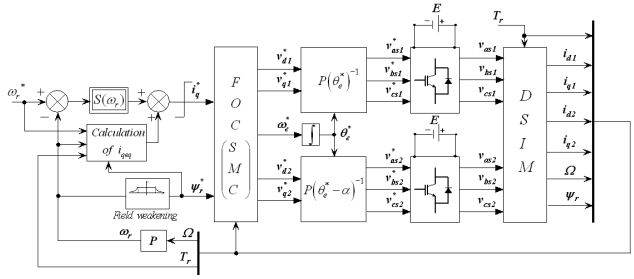

Fig. 3. Indirect FOC scheme for DSIM.

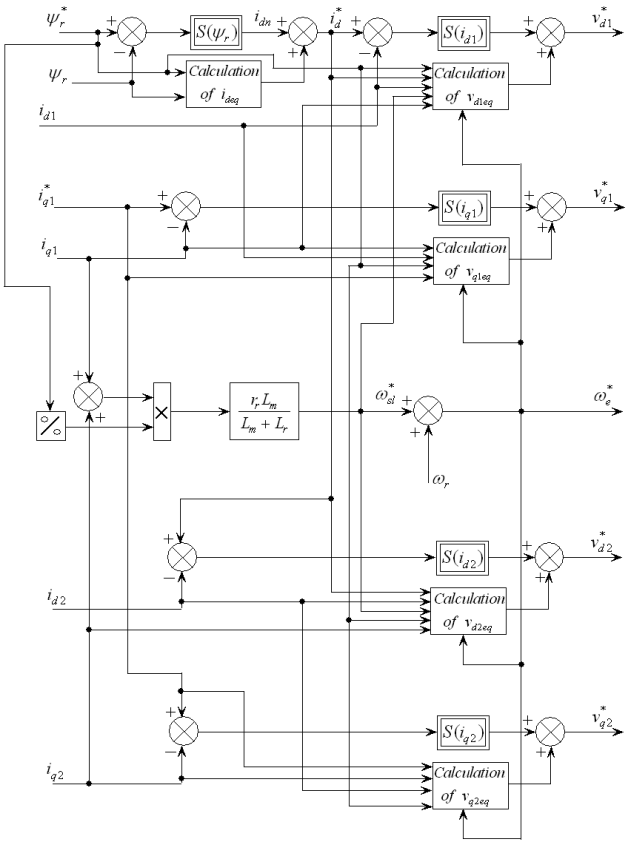

Fig. 4. Bloc diagram of the FOC(SMC).

B. Development of the Control Laws

By using the equations systems (28)-(33), (37) and (45), the regulators control laws are obtained as follows:

1) For the Speed Regulator:

$$S(\omega_r)\dot{S}(\omega_r) < 0 \Rightarrow \imath_q^* = \imath_{qeq} + \imath_{qn} \tag{52}$$

with

$$\imath_q = \imath_{q1} + \imath_{q2} \quad \text{and} \quad \omega_r = P\Omega;$$

$$\imath_{qeq} = \frac{J}{P^2}\frac{L_r + L_m}{L_m \psi_r^*} + \left[\dot{\omega}_r^* \frac{f}{J}\omega_r + \frac{P}{J}T_r\right];$$

$$\imath_{qn} = k_{\omega_r}\frac{S(\omega_r)}{|S(\omega_r)| + \xi_{\omega_r}}.$$

2) For the Flux Regulator:

$$S(\psi_r)\dot{S}(\psi_r) < 0 \Rightarrow \imath_d^* = \imath_{deq} + \imath_{dn} \tag{53}$$

where

$$\imath_d = \imath_{d1} + \imath_{d2};$$

$$\imath_{deq} = \frac{L_r + L_m}{r_r L_m}\left[p\psi_r^* + \frac{r_r}{L_r + L_m}\psi_r\right];$$

$$\imath_{dn} = k_{\psi_r}\frac{S(\psi_r)}{|S(\psi_r)| + \xi_{\psi_r}}.$$

3) For the Stator currents:

$$S(\imath_{d1})\dot{S}(\imath_{d1}) < 0 \Rightarrow v_{d1}^* = v_{d1eq} + v_{d1n} \tag{54}$$

$$S(\imath_{q1})\dot{S}(\imath_{q1}) < 0 \Rightarrow v_{q1}^* = v_{q1eq} + v_{q1n} \tag{55}$$

$$S(\imath_{d2})\dot{S}(\imath_{d2}) < 0 \Rightarrow v_{d2}^* = v_{d2eq} + v_{d2n} \tag{56}$$

$$S(\imath_{q2})\dot{S}(\imath_{q2}) < 0 \Rightarrow v_{q2}^* = v_{q2eq} + v_{q2n} \tag{57}$$

with

$$v_{d1eq} = L_1 i_{d1}^* + r_1 \imath_{d1} - \omega_e^*\left[L_1 \imath_{q1} + \tau_r \psi_r^* \omega_{sl}^*\right];$$

$$v_{q1eq} = L_1 i_{q1}^* + r_1 \imath_{q1} + \omega_e^*\left[L_1 \imath_{d1} + \psi_r^*\right];$$

$$v_{d2eq} = L_2 i_{d2}^* + r_2 \imath_{d2} - \omega_e^*\left[L_2 \imath_{q2} + \tau_r \psi_r^* \omega_{sl}^*\right];$$

$$v_{q2eq} = L_2 i_{q2}^* + r_2 \imath_{q2} + \omega_e^*\left[L_2 \imath_{d2} + \psi_r^*\right];$$

and

$$v_{d1n} = k_{d1}\frac{S(\imath_{d1})}{|S(\imath_{d1})| + \xi_{d1}};$$

$$v_{q1n} = k_{q1}\frac{S(\imath_{q1})}{|S(\imath_{q1})| + \xi_{q1}};$$

$$v_{d2n} = k_{d2}\frac{S(\imath_{d2})}{|S(\imath_{d2})| + \xi_{d2}};$$

$$v_{q2n} = k_{q2}\frac{S(\imath_{q2})}{|S(\imath_{q2})| + \xi_{q2}}.$$

To satisfy the stability condition of the system, the gains k_{ω_r}, k_{ψ_r}, k_{d1}, k_{q1}, k_{d2} and k_{q2} should be taken positive by selecting the appropriate values [19].

VI. Simulation Results and Discussion

The dual-stator induction motor parameters used in the simulation are given in the Appendix.

The first test concerns a no-load starting of the motor with a reference speed $n^* = 2500rpm$. Then a torque load $T_L = 14N.m$ is applied between $t = 1.5sec$ and $t = 2.5sec$. The results are shown in Fig. 5.

The second test concerns a no-load starting of the motor with a reference speed $n^* = 2500rpm$. Then at $t = 1.5sec$ a reverse speed is applied. The results are shown in Fig. 6.

It is noticed that the speed regulation is obtained using such as controller is spite of the presence of stern disturbances such as step change of the load torque.

The waveforms depicted in Fig. 5 show that the ideal field-oriented control is established by setting the flux responses $\psi_{dr} = 1Wb$, $\psi_{qr} = 0Wb$, despite the load variations. The step changes in the load torque and the reverse of speed response cause step change in the torque response without any effects on the fluxes responses, which are maintained constant, due to the decoupled control system between the torque and the rotor flux. Thus, the aim of the field-oriented control is achieved, and the introduction of perturbations is immediately rejected by the control system.

The aim of the third test is to solve the problem of detuning in indirect field-oriented control system in the case of parameter variations of the motor. The coefficients in equations systems (28)-(33) are all dependent on the motor parameters.

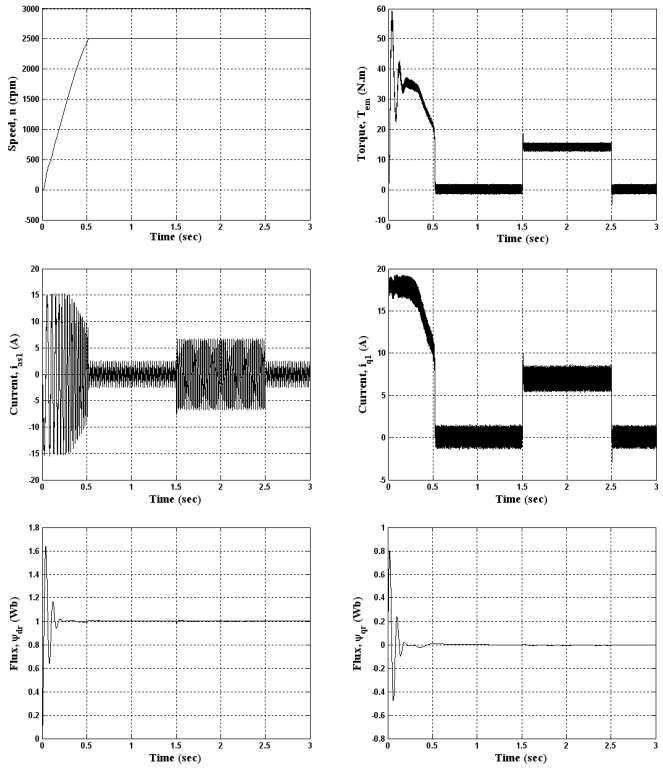

Fig. 5. Simulation results for a cascade structure using SMCs.

These parameters may vary during on-line operation due to temperature or saturation effects. So, it is important to investigate the sensitivity of the complete system to parameters changes.

One of the most significant parameter changes in the motor is the rotor resistance r_r. A simulation taking into account the variation of 100% rise of r_r relative to the identified model parameter was carried out. The parameters changes are introduced only in the model of the motor. Neither the estimator, nor the controller is involved by this variation. The waveforms obtained are illustrated in Fig. 7. The responses are approximately similar to chose obtained in Fig. 5 and the condition of oriented control is obtained in the steady state ($\psi_{qr} = 0Wb$). It can be conclude that the proposed sliding controllers are robust. They are able to realize and maintain the control even the parameters of the motor (r_r) change.

VII. Conclusion

In this paper, a sliding mode control strategy of the dual-stator induction motor drives has been presented. This control methodology has the property of imposing the control signal necessary to enforce the desired feedback control law independently of model uncertainties.

The effectiveness of the proposed controllers has been demonstrated by simulation and successfully implemented in an dual-stator induction motor drives.

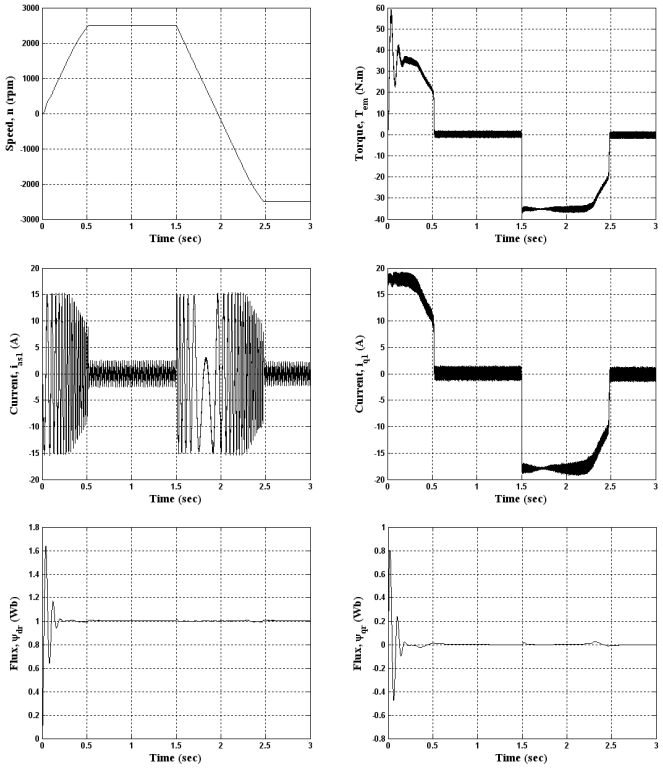

Fig. 6. Simulation results for a cascade structure using SMCs, with reverse speed at $t = 1.5sec$.

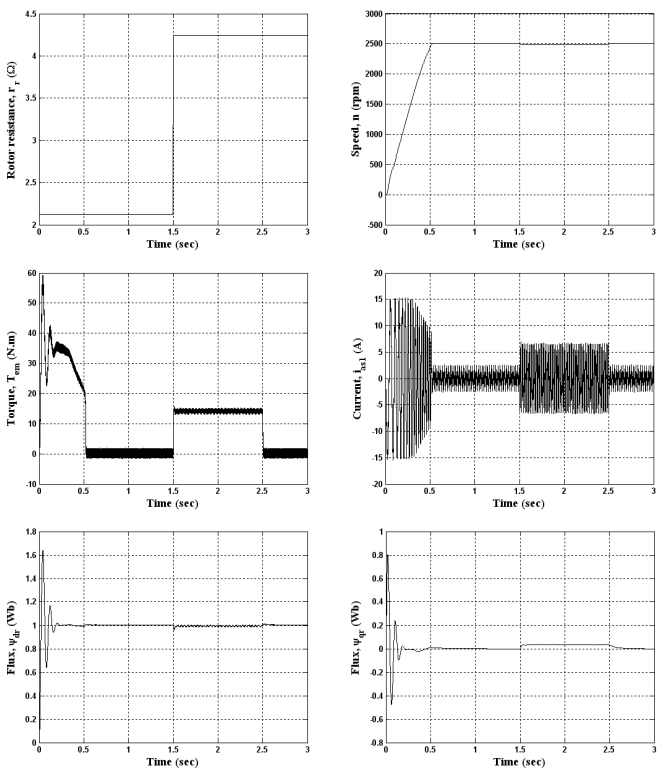

Fig. 7. Simulation results with variation of 100% of r_r for an indirect FOC drive with SMCs.

APPENDIX

The machine parameters used in the simulation are as follows:

- Stator resistances (winding set I and II) $r_1 = r_2 = 3.72\Omega$;
- Stator self inductances (winding set I and II) $L_1 = L_2 = 0.022H$;
- Rotor resistance $r_r = 2.12\Omega$;
- Rotor self inductance $L_r = 0.006H$;
- Mutual inductance between stator and rotor $L_m = 0.3672H$;
- Moment of inertia $J = 0.0625kg.m^2$;
- Viscous bearing friction coefficient $f = 0.001N.m.s/rd$.

REFERENCES

[1] P. L. Alger and R. E. Arnold, "The history of induction motors in America," *in Proc. IEEE*, vol. 64, no. 9, Sep. 1976, pp. 1380–1383.

[2] Y. Zhao and T. A. Lipo, "Space vector PWM control of dual three-phase induction machine using vector space decomposition," *IEEE Trans. Ind. Appl.*, vol. 31, no. 5, pp. 1100–1109, Sep./Oct. 1995.

[3] D. Hadiouche, H. Razik and A. Rezzoug, "On the modeling and design of dual-stator windings to minimize circulating harmonic currents for VSI fed AC machines," *IEEE Trans. Ind. Appl.*, vol. 40, no. 2, pp. 506–515, Mar./Apr. 2004.

[4] R. Bojoi, A. Tenconi, G. Griva and F. Profumo, "Vector control of dual-three-phase induction-motor drives two current sensors," *IEEE Trans. Ind. Appl.*, vol. 42, no. 5, pp. 1284–1292, Sep./Oct. 2006.

[5] E. A. Klingshirn, "High phase order induction motors-part I-description and theoretical considerations," *IEEE Trans. Power App. Syst.*, vol. PAS–102, no. 1, pp. 47–53, Jan. 1983.

[6] E. Levi, "Recent developments in high performance variable speed multiphase induction motor drives," *in Sixth Int. Symposium Nikola Tesla*, Belgrade, SASA, Serbia, Oct. 18–20, 2006.

[7] V. I. Utkin, "Variable structure systems with sliding modes," *IEEE Trans. Autom. Control*, vol. AC–22, no. 2, pp. 212–222, Apr. 1977.

[8] S. J. Huang and H. Y. Chen, "Adaptive sliding controller with self-tuning fuzzy compensation for vehicle suspension control," *ScienceDirect*, Elsevier, Mechatronics 16, pp. 607–622, 2006.

[9] Z. Yan, C. Jin and V. I. Utkin, "Sensorless sliding-mode control of induction motors," *IEEE Trans. Ind. Electron.*, vol. 47, no. 6, pp. 1286–1297, Dec. 2005.

[10] D. Hadiouche, "Contribution to the study of dual stator induction machines : Modeling, supplying and structure," (in french), Ph.D. dissertation, GREEN, Faculty Sci. Tech. Univ. Henri Poincar-Nancy I, Vandoeuvre-lès-Nancy, France, Dec. 2001.

[11] H. Amimeur, R. Abdessemed, D. Aouzellag, E. Merabet and F. Hamoudi,, "Modeling and Analysis of Dual-Stator Windings Self-Excited Induction Generator," *Journal Elec. Engineering JEE*, art. 3, iss. 3, vol. 8, 2008.

[12] G. K. Singh, K. Nam and S. K. Lim, "A simple indirect field-oriented control scheme for multiphase induction machine," *IEEE Trans. Ind. Electron.*, vol. 52, no. 4, pp. 1177–1184, Aug. 2005.

[13] D. Berbier, E. M. Berkouk, A. Talha and M. O. Mahmoudi, "Study and control of two two-level PWM rectifiers-clamping bridge-two three-level NPC VSI cascade. Application to double stator induction machine," *in 35th Annual IEEE Power Electron. Specialists Conf.*, Aachen, Germany, 2004, pp. 3894–3899.

[14] Z. Oudjebour, E. M. Berkouk, N. Sami, S. Belgasmi, S. Arezki and I. Messaif, "Indirect space vector control of a double star induction machine fed by two five-levels NPC VSI," *in Int. Conf. Elec. Mach.*, ICEM'04, Poland, 2004.

[15] E. Merabet, R. Abdessemed, H. Amimeur and F. Hamoudi, "Field oriented control of a daul star induction machine using fuzzy regulators," *in 4th Int. Conf. Computer Integrated Manufacturing*, CIP'07, Paper Ref: F10, Univ. Setif, Algeria, Nov. 03–04, 2007.

[16] A. Hazzab, I. K. Bousserhane and M. Kamli, "Design of a fuzzy sliding mode controller by genetic algorithms for induction machine speed control," *Int. Journal Emerging Elec. Power Syst.*, vol. 1, iss. 2, art. 1008, pp. 1–17, 2004.

[17] M. F. Benkhoris and A. Gayed, "Discrete sliding control technique of DC motor drive," *in IEE Conf. publication Power Electron. Variable Speed drives*, no. 429, Sep. 23–25, 1996, pp. 81–86.

[18] S. Bouabdallah and R. Siegwart, "Backstepping and sliding-mode techniques applied to an indoor micro quadrotor," *in Proc. IEEE Int. Conf. Robotics Automation*, Barcelona, Spain, Apr. 2005, pp. 2259–2264.

[19] L. Barazane, M. L. Benzaoui and R. Ouiguini, "A fuzzy sliding mode control associated to the field-oriented control of asynchronous motor," *in 4th Int. Conf. Elec. Engineering*, CEE'06, Batna, Algeria, Nov. 7-8, 2006, pp. 117–123.